Additional file 1 for

Enhanced Chemotherapy Response in Hepatocellular Carcinoma: Synergistic Effects of miR-122 and Doxorubicin Co-Delivery System Inducing Apoptosis and DNA Damage

Table S1. The information of DNA sequences in this work：

Name	Sequences (5'-3')
miRNA 122	GAGTGTGACAATGGTGTTTG
CTRL-122	GACTACGACATGAATCTTCG
miRNA 122-Cy5	GAGTGTGACAATGGTGTTTG

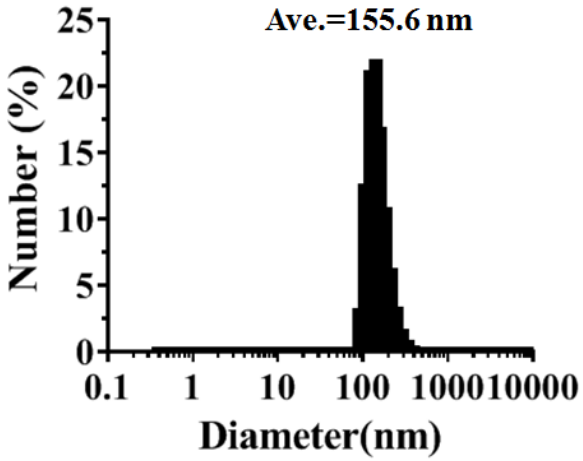

Fig S1. DLS measurement of Fe-miR122/DOX.

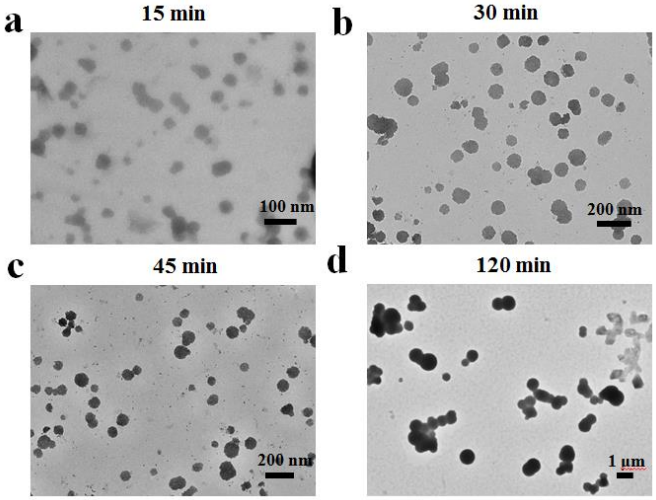

Fig S2. The TEM images of Fe-miR122/DOX at different reaction times.

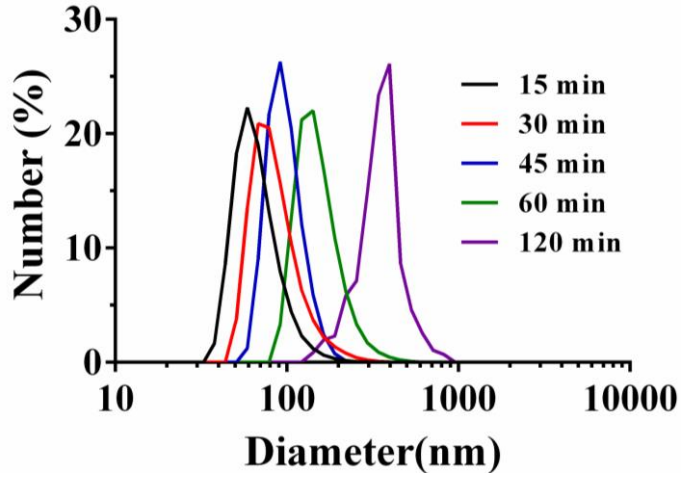

Fig S3. DLS measurement of Fe-miR122/DOX at different reaction times.

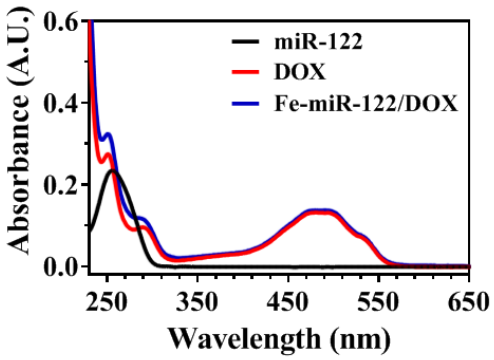

Fig S4.UV-visble absorption spectroscopy of miR-122, DOX and Fe-miR122/DOX.

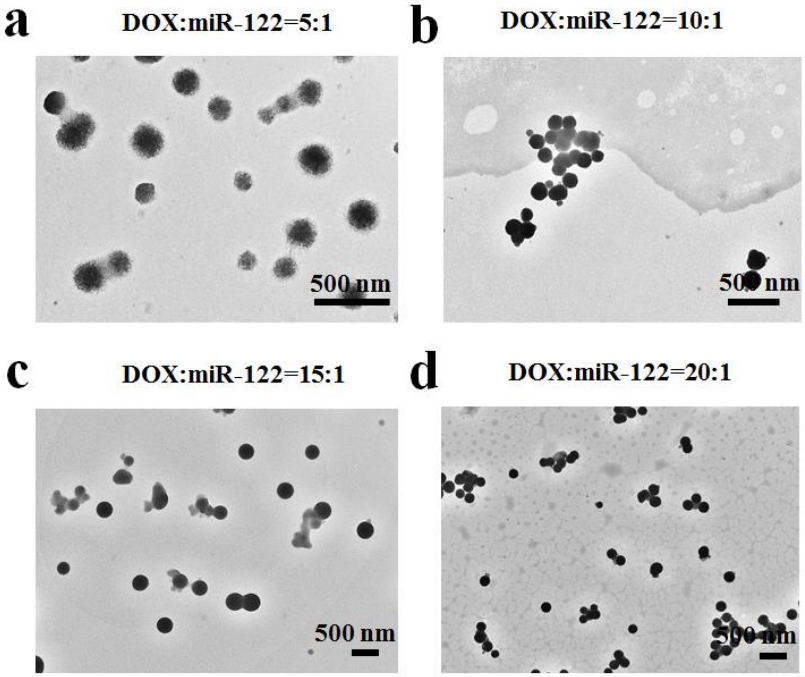

Fig S5. TEM images of Fe-miR122/DOX synthesized with different DOX: miR122 ratios: (a) 5:1, (b) 10:1, (c) 15:1 and (d) 20:1. Scale bar=500 nm.

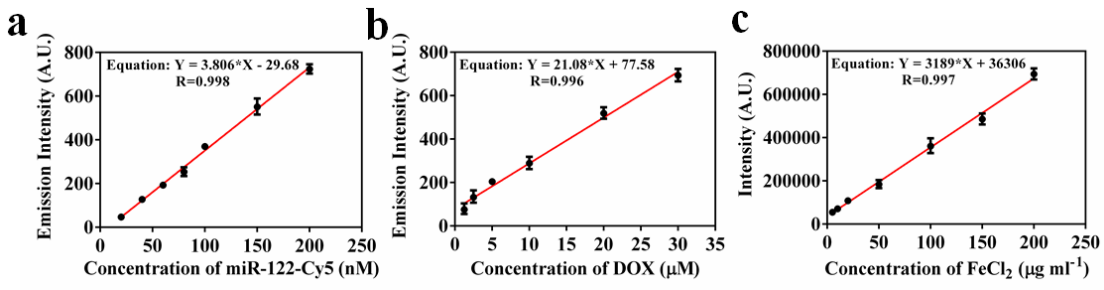

Fig S6. Standard curves of fluorescence intensity versus concentration for miR122-Cy5 at 665 nm (a), DOX at 592 nm (b), and emission intensity versus concentration standard curve for ICP-MS quantification of Fe ions preparation concentration (c). miR122-Cy5 excitation at 635 nm, DOX excitation at 488 nm (n=3).

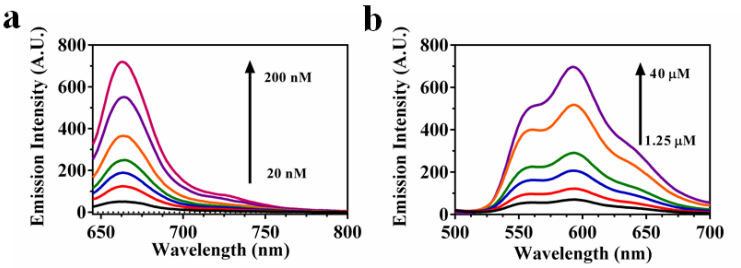

Fig S7. Fluorescence response of (a) miR122-Cy5 and (b) DOX.

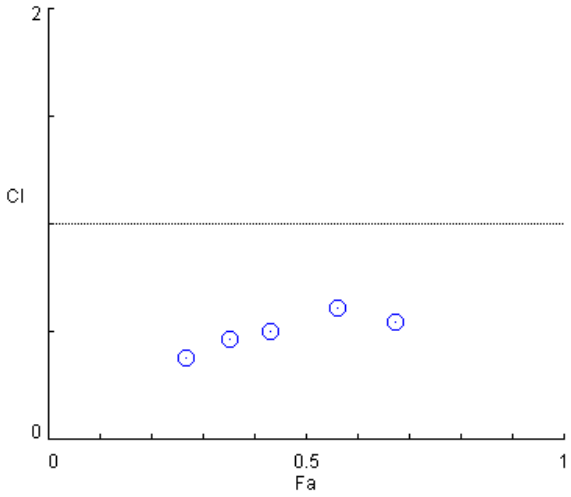

Fig S8. The combination index (CI) of DOX and miR-122 at 10:1, 15:1, 20:1, 30:1 and 40:1 was evaluated by Chou-Talalay method.

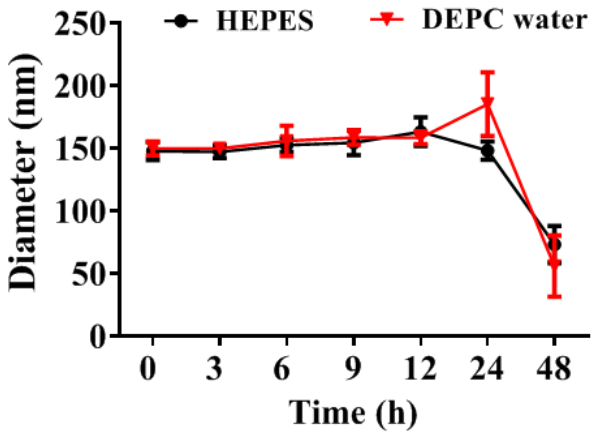

Fig S9. The diameter of Fe-miR-122/DOX nanoparticles measured by DLS at different times (n=3).

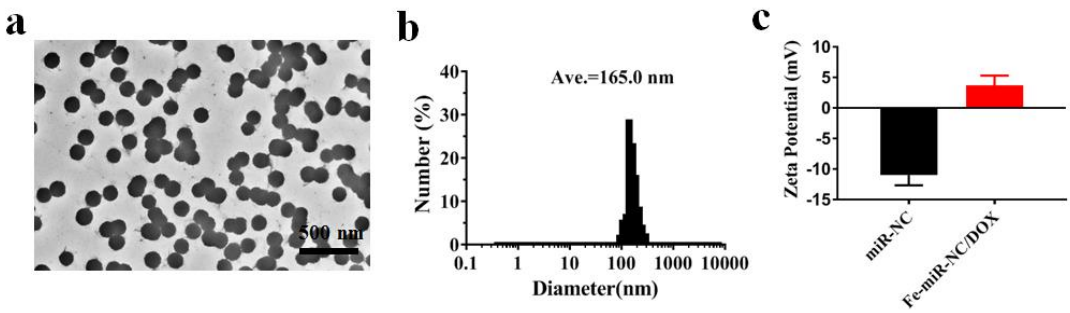

Fig S10. TEM images (a), DLS measurement (b) and Zeta potential analysis (c) of Fe-miR-NC/DOX at 60 min.

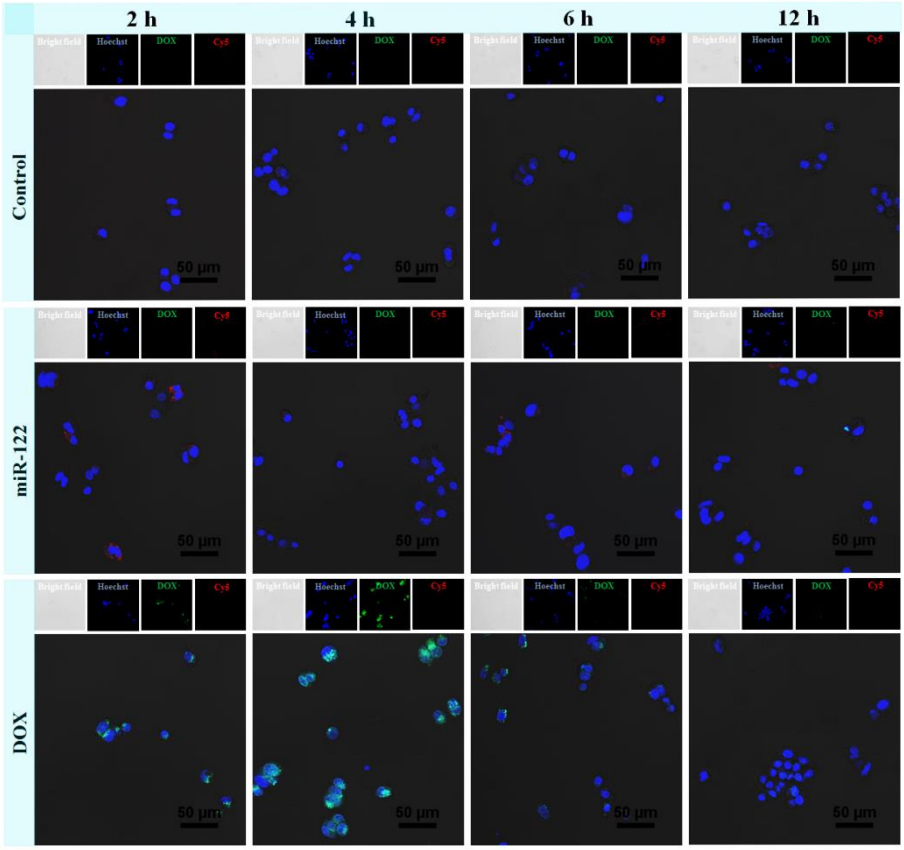

Fig S11. CLSM images of HepG2 cells treated with PBS, miR-122 and DOX for different time.

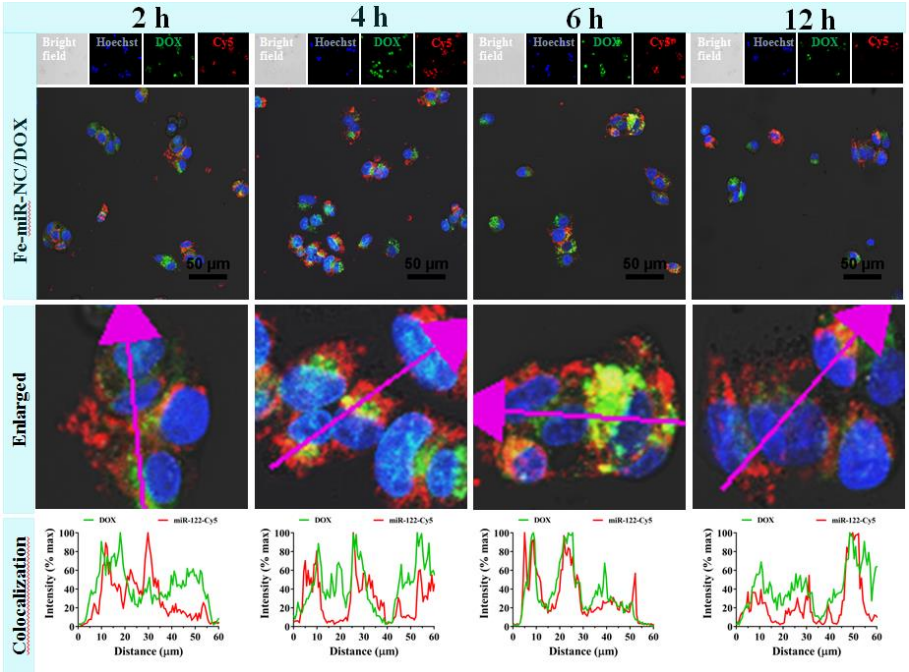

Fig S12. CLSM images of HepG2 cells treated with Fe-miR-NC/DOX for different time and fluorescent intensity of DOX and miR122-Cy5 signals across 60 μm regions marked with arrows is shown in line plots.

	2 h	4h	6h	12 h
Fe-miR-NC-Cy5/DOX	**0.640**	**0.652**	**0.662**	**0.601**
Fe-miR-122-Cy5/DOX	**0.682**	**0.668**	**0.655**	**0.596**

Fig S13. Pearson correlation coefficients between miR-122-Cy5 (red) and DOX (green) fluorescence signals at different time points.

	2 h	4h	6h	12 h
Fe-miR-122/DOX	**0.695**	**0.636**	**0.509**	**0.467**

Fig S14. Pearson correlation coefficients between lysosomal (red) and DOX (green) fluorescence signals at different time points.

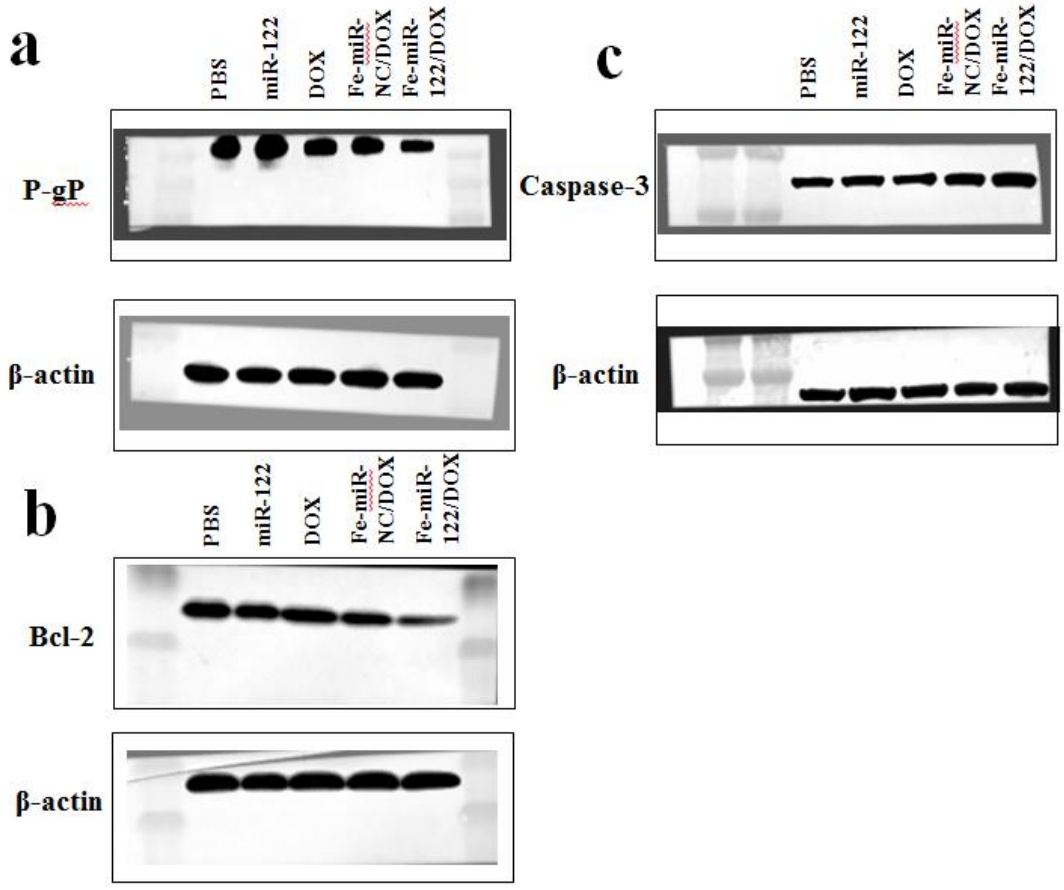

Fig S15. Unaltered raw Western blot data displaying (a) P-gP, (b) Bcl-2, (c) Caspase-3 and their corresponding β-actin controls as depicted in Fig. 6a.

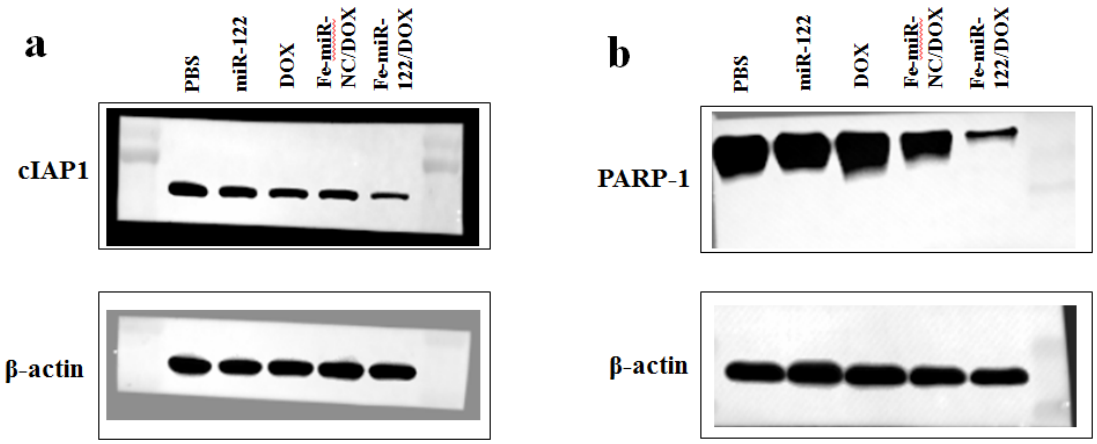

Fig S16. Unaltered raw Western blot data displaying (a) cIAP1, (b) PARP-1 and their corresponding β-actin controls as depicted in Fig. 6c. In the WB analysis, it is important to note that P-gp and cIAP1 were resolved on the same gel, which allowed for the β-actin to appear as a single band. Therefore, the β-actin images shown in Fig S15a and Fig S16a are derived from the same gel.

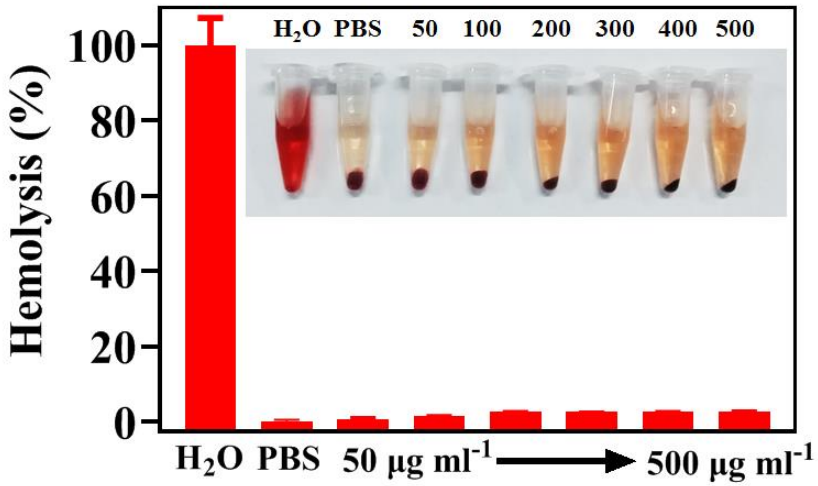

Fig S17 Hemolysis experiment determination of Fe-miR-122/DOX hemolysis of red blood cells in whole blood effect.